

Par-complex proteins promote proliferative progenitor divisions in the developing mouse cerebral cortex

Marcos R. Costa¹, Gaiping Wen¹, Alexandra Lepier², Timm Schroeder¹ and Magdalena Götz^{1,2,*}

The size of brain regions depends on the balance between proliferation and differentiation. During development of the mouse cerebral cortex, ventricular zone (VZ) progenitors, neuroepithelial and radial glial cells, enlarge the progenitor pool by proliferative divisions, while basal progenitors located in the subventricular zone (SVZ) mostly divide in a differentiative mode generating two neurons. These differences correlate to the existence of an apico-basal polarity in VZ, but not SVZ, progenitors. Only VZ progenitors possess an apical membrane domain at which proteins of the Par complex are strongly enriched. We describe a prominent decrease in the amount of Par-complex proteins at the apical surface during cortical development and examine the role of these proteins by gain- and loss-of-function experiments. Par3 (Pard3) loss-of-function led to premature cell cycle exit, reflected in reduced clone size *in vitro* and the restriction of the progeny to the lower cortical layers *in vivo*. By contrast, Par3 or Par6 (Pard6 α) overexpression promoted the generation of Pax6⁺ self-renewing progenitors *in vitro* and *in vivo* and increased the clonal progeny of single progenitors *in vitro*. Time-lapse video microscopy revealed that a change in the mode of cell division, rather than an alteration of the cell cycle length, causes the Par-complex-mediated increase in progenitors. Taken together, our data demonstrate a key role for the apically located Par-complex proteins in promoting self-renewing progenitor cell divisions at the expense of neurogenic differentiation in the developing cerebral cortex.

KEY WORDS: Cortical progenitors, Cell lineage, Cell proliferation, Pax6, Tbr2 (Eomes)

INTRODUCTION

The size of different brain regions depends on the size of the progenitor pool, which is in turn determined by the number of symmetric proliferative cell divisions. This concept, formulated by Rakic (Rakic, 1988), tries to explain the enlargement of the cerebral cortex observed during evolution as well as the differences in size of distinct brain areas. It is predicted that the number of symmetric proliferative divisions determines the progenitor pool and thereby the size of the cerebral cortex, whereas the number of differentiative divisions generating either one or two neurons determines the number of neurons per surface area, i.e. the thickness of the cerebral cortex. Indeed, this concept has been well supported through the identification of sets of progenitors dividing mostly in a proliferative mode (neuroepithelial cells) and others mostly in a differentiative mode (basal progenitors).

Prior to neurogenesis, neuroepithelial cells divide exclusively in the symmetric proliferative mode, giving rise to two progenitor cells (Chenn and McConnell, 1995). At the onset of neurogenesis, two sets of progenitors arise, the apically located radial glial cells forming the ventricular zone (VZ) and the basally located subventricular zone (SVZ) cells. The latter largely divide in a symmetric differentiative mode generating two postmitotic neurons (Miyata et al., 2004; Haubensak et al., 2004; Noctor et al., 2004). By contrast, radial glial cells located in the VZ either divide in a symmetric proliferative mode or divide asymmetrically, generating a radial glial cell and a postmitotic neuron or a basal progenitor cell

(Noctor et al., 2001; Noctor et al., 2004; Miyata et al., 2001; Miyata et al., 2004; Tamamaki et al., 2001) and thereby contributing to the generation of neurons destined for different cortical layers (Takahashi et al., 1999; Desai and McConnell, 2000; Shen et al., 2006). Thus, during cortical neurogenesis, distinct sets of progenitors contribute differently to the differentiative and proliferative cell divisions, suggesting that the generation of these specific types of progenitors might actually regulate the size and thickness of the cerebral cortex. Indeed, considerably enlarged upper cortical layers characterize the primary visual area of the cortex in primates (for a review, see Dehay and Kennedy, 2007). They are formed by basal SVZ progenitors as this layer dominates the progenitor pool during the formation of the upper cortical layers (Smart et al., 2002; Lukaszewicz et al., 2005). Moreover, faster cell cycle kinetics regulate the enlargement of the primary visual area as compared with other neighboring cortical areas in primates (Lukaszewicz et al., 2005). Thus, the speed of the cell cycle and the type of cortical progenitors appear to be critical for the size and thickness of the cortex or of a specific cortical area. However, although the dynamic progression in the cellular composition of the developing cerebral cortex has been extensively examined, the molecular mechanisms controlling the generation of specific progenitor subtypes and their mode of cell division are not well understood.

One of the molecular characteristics distinguishing the apically located VZ progenitors from the basally located SVZ progenitors is their apico-basal polarity. The VZ progenitors are highly polarized (for a review, see Götz and Huttner, 2005), with an apical domain enriched in the Par-complex proteins Par3, Par6, aPKC λ (also known as Pard3, Pard6 α and Prkci, respectively – Mouse Genome Informatics) and Cdc42 (Manabe et al., 2002; Kosodo et al., 2004; Cappello et al., 2006; Imai et al., 2006; von Trotha et al., 2006; Afonso and Henrique, 2006; Kovac et al., 2007) that is separated from the basolateral membrane domain by adherens junctions (Mollgard et al., 1987; Astrom and Webster, 1991) (for a review, see

¹GSF- National Research Institute for Environment and Health, Institute for Stem Cell Research, Ingolstädter Landstr. 1, 85764 Neuherberg/Munich, Germany.

²Physiological Genomics, University of Munich, Schillerstr. 46, 80639 Munich, Germany.

*Author for correspondence (e-mail: Magdalena.goetz@gsf.de)

Götz and Huttner, 2005). By contrast, the basal SVZ progenitors display none of these features. Unlike in *Drosophila*, however, the role of apico-basal polarity and adherens junctions in vertebrate VZ and SVZ progenitor cell division has not yet been elucidated (reviewed by Wodarz and Huttner, 2003).

Recently, it has been shown that conditional deletion of *Cdc42* in early VZ progenitors leads to an increased number of basal *Tbr2*-positive progenitors (*Tbr2* is also known as *Eomes* – Mouse Genome Informatics) and a premature increase in neuron production (Cappello et al., 2006). As *Cdc42* is well known to activate the apically localized Par complex, we proposed that the Par complex might contribute to maintain apical progenitors, thereby promoting symmetric proliferative or asymmetric cell divisions. However, the rate of neuron generation remained unaffected when aPKC λ (a Par-complex protein) was inactivated at later developmental stages (Imai et al., 2006). Two explanations could account for these observations: either *Cdc42* does not act via the Par complex to increase basal progenitors, or the Par complex plays a prominent role only at earlier developmental stages. We were therefore prompted to examine the expression levels of Par proteins during corticogenesis and elucidate their function by *Par3* and *Par6* gain- or loss-of-function experiments *in vitro* and *in vivo*.

MATERIALS AND METHODS

Animals

C57/Bl/6J mice, obtained from Charles River, were maintained on a 12-hour (07.00 to 19.00 h) light-dark cycle. The day of the vaginal plug was considered as E0 and the day of birth as P0. All experimental procedures were performed in accordance with Society for Neuroscience and European Union guidelines and were approved by our institutional animal care and utilization committees.

Plasmids

The full-length cDNA of *Par3* (accession number AY_026057) and *Par6* alpha (accession number NM_019695) were cloned into the retroviral plasmid pMXIG (Mizuguchi et al., 2001). The short-hairpin RNA (shRNA) duplexes were designed against the full-length cDNA of *Par3*. They contain the respective sequence in sense orientation, followed by eight nucleotides CAAGCTTC as loop, followed by the respective sequence in antisense orientation and six nucleotides T as termination. The synthesized double-stranded DNA nucleotides were annealed and ligated into pbs-U6 plasmid with same cloning site immediately downstream of the U6 promoter. The U6-shRNA cassette was generated by PCR using the forward primer U6_E22 (5'-GCAGGAATCCCTGCAGGCATGCAAGCG-3') and the reverse primer U6_C22 (5'-CGGTATCGATGCTCTAGAACTAGGATTGGC-3') containing *EcoRI* and *Clal* sites and subcloned into the lentiviral plasmid pLVTH (Wiznerowicz and Trono, 2003) after deleting the H1 promoter. The three oligonucleotides designed were *Par3a* (5'-GGAGATCTTCGAAACAGAAGA-3'; 21 bp), *Par3b* (5'-GCAGCAAACAAGGAGCAATAT-3'; 21 bp) and *Par3c* (5'-GAAGAAAGTAGGCAAGAGGCT-3'; 21 bp).

Virus production

Replication-incompetent enhanced-GFP-expressing retrovirus was produced from a stably transfected packaging cell line (GPG-293) transiently transfected with the retroviral expression plasmid. Lentiviral vectors were produced by transient cotransfection of 293T cells with the following plasmids: lentiviral packaging plasmid pCMVdelta8.9, pseudotyping plasmid pSVVG (both kindly provided by Pavel Osten, Northwestern University, Feinberg Medical School, Chicago, IL) and lentiviral expression plasmid. Supernatant was harvested 48 and 72 hours after transfection, centrifuged at low speed and filtered through a 0.45 μ m low-protein-binding PVDF filter (Millipore). Viral particles were pelleted at 50,000 *g* at 4°C for 2 hours, resuspended in a large volume of TBS-5 (50 mM Tris-HCl pH 7.8, 130 mM NaCl, 10 mM KCl, 5 mM MgCl₂) and stored at -80°C.

Histology and immunohistochemistry

Timed pregnant mice were sacrificed by cervical dislocation. Embryonic brains were removed and fixed in 4% paraformaldehyde (PFA) in PBS, cryoprotected in 30% sucrose solution (in PBS), embedded in Tissue-tek and cryosectioned (20-30 μ m).

Sections or coverslips (see below) were incubated in primary antibody overnight at 4°C in 0.5% Triton X-100 and 10% normal goat serum in PBS. Primary antibodies were: anti-*Par3* (rabbit, Upstate, 1:500), anti-aPKC λ (mouse, BD Transduction, 1:200), anti-pan-cadherin (mouse, Sigma, 1:100), anti-Ki67 (rat, Dako, 1:50), anti-*Tbr2* (rabbit, Chemicon, 1:100), anti-*Pax6* (rabbit, Chemicon, 1:750), anti-*Tbr1* (rabbit, Chemicon, 1:100), anti- β III-tubulin (mouse IgG2b, Sigma, 1:100), anti-MAP2 (mouse IgG1, Sigma, 1:100), anti-GFP (rabbit, Clontech, 1:500; chicken, Sigma, 1:500), anti-*nestin* (mouse IgG1, Hybridoma Bank, 1:10). Nuclei were visualized by incubating sections for 10 minutes with 0.1 μ g/ml DAPI (4',6' diamidino-2-phenylindole, Sigma) in PBS. Fluorescent secondary antibodies were used according to the manufacturer's protocol (Jackson ImmunoResearch or Southern Biotechnologies). Sections or coverslips were mounted in Aqua Polymount (Polyscience) and analyzed using Zeiss Axioplan 2 and Olympus confocal laser-scanning microscopes.

In-utero injection

E12- and E13-timed pregnant mice were anaesthetized with a mixture of fentanyl (0.05 mg/kg), midazolam (5 mg/kg) and metedomidine (0.5 mg/kg). Only when deep anesthesia was verified by the absence of pain reflexes were the uterine horns exposed after caesarean incision. Under fiber optic lighting, each embryo was manipulated through the uterine wall until the position of the lateral ventricle was discernible. Viral vector suspension (0.5 \pm 1.0 μ l) with Fast Green (2.5 mg/ μ l, Sigma) was injected into the cerebral ventricles through a bevelled glass micropipette. After injection, the peritoneal cavity was rinsed with warmed 0.9% NaCl, the uterine horns were replaced and the wound was closed. Anesthesia was terminated by injection of naloxon (1.2 mg/kg), flumazenil (0.5 mg/kg) and atipamezol (2.5 mg/kg). Post-operative care involved application of painkillers and surveillance several times a day. Animals recovered very well after the operation and no signs of distress could be observed 1 day later.

Primary cell culture

Embryonic brains were isolated from E12-14 timed pregnant mice. The lateral portion of the dorsal telencephalon was dissected and dissociated as described previously (Heins et al., 2001). After 2 hours, cultures were infected with a low titer (<30 particles) of the viruses described above and medium changes and fixation after 7 days *in vitro* were performed as previously described (Heins et al., 2001).

By using a low number of viral particles to transduce the cells, we could identify well-separated cell clusters at 20 \times magnification and the mean number of clusters per coverslip in the experiments described was found to be 24.7 \pm 9.2 (mean \pm s.e.m.). This allowed us to infer that each cluster was derived from a single progenitor cell and could therefore be defined as an individual clone (Williams et al., 1991; Haubst et al., 2004). This was also confirmed by time-lapse video microscopy. The mean number of neuronal and non-neuronal cells within different types of clones, as well as the frequency of clones with a given size, were plotted and are shown as mean \pm s.e.m. Data were derived from at least three experimental batches with four to six coverslips analyzed per experiment.

Time-lapse video microscopy

Primary E12/13 cortical cell cultures were prepared as described above and infected with a greater number of virus particles. Twenty hours after viral infection and 2 hours after medium replacement, the tissue culture plate was tightly sealed and time-lapse microscopy was performed with a cell observer (Zeiss) at a constant 37°C. Phase-contrast images were acquired every 2 minutes and fluorescence images every 3 hours for 5 days with Axiovision Rel. 4.5 software (Zeiss) and an AxioCam HRm camera. Images were assembled into a movie and analyzed using Axiovision Rel. 4.5 and MetaMorph Offline (Version 6.1r4, Molecular Devices) software. Transduced cells were recognized by GFP fluorescence and tracked in phase-contrast images, enabling the identification of single-cell lineages.

RESULTS

A decrease in apically localized components of the Par complex during cortical development

We first analyzed the expression of the Par-complex proteins Par3 and aPKC λ in the embryonic cortex at different developmental stages. Consistent with previous data (Manabe et al., 2002; Kosodo et al., 2004; Cappello et al., 2006), we observed a strong enrichment of Par3, Par6 and aPKC λ immunoreactivity at the apical surface of the VZ at E12 (Fig. 1A-C,G-I,M-O). The expression level gradually weakened at subsequent developmental stages (E14, data not shown) and was almost absent by E16 (Fig. 1D-F,J-L,P-R). This decrease in Par3, Par6 and aPKC λ -immunoreactivity at the apical

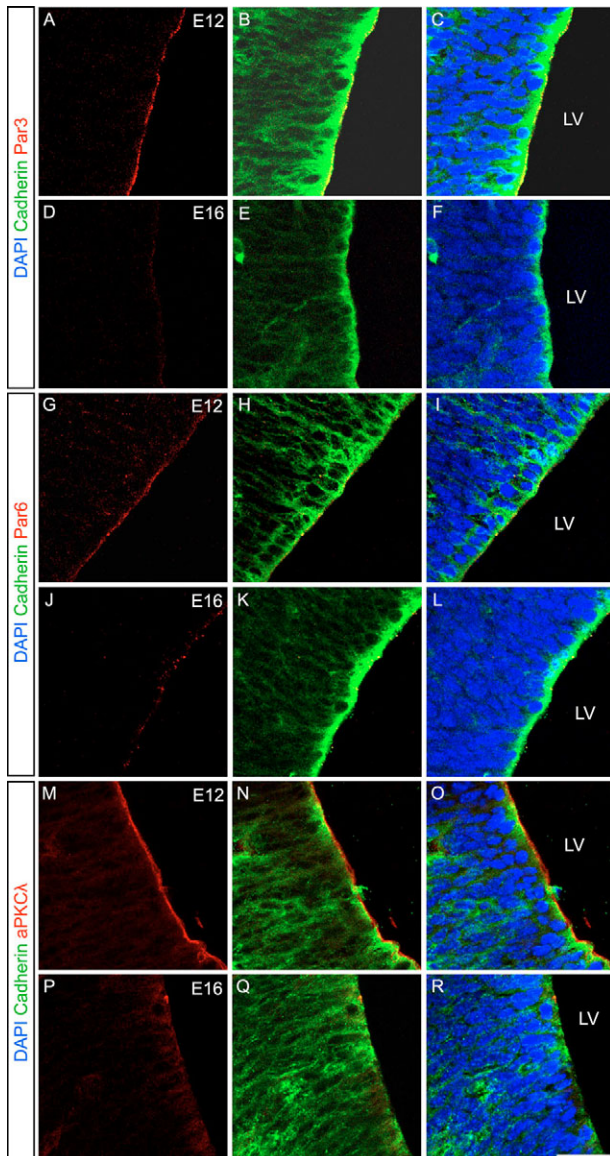


Fig. 1. Par-complex proteins are reduced at the ventricular surface during cortical neurogenesis. (A-R) Coronal section through E12 (A-C,G-I,M-O) and E16 (D-F,J-L,P-R) mouse cerebral cortices immunolabeled for Par3 (A-F, red), Par6 (G-L, red) or aPKC λ (M-R, red), pan-cadherin (green) and stained with DAPI (blue). Note the high immunoreactivity for Par3, Par6 and aPKC λ in the apical domain of the VZ at E12 and its reduction at later developmental stages. Scale bar: 25 μ m.

surface correlates with the decrease in proliferative cell divisions towards mid-neurogenesis (E14-16) in the developing cortex (Takahashi et al., 1995; Chenn and McConnell, 1995; Haydar et al., 2003; Noctor et al., 2004; Haubensak et al., 2004).

Par3 knockdown decreases clone size in vitro

The continuing decrease in Par3 expression during development prompted us to examine a potential role for this complex in VZ progenitors by reducing Par3 protein. We targeted three different regions of *Par3* with short hairpin sequences (see Materials and methods), one of which had previously been shown to mediate successful knockdown of the protein (Plusa et al., 2005). A reduction in Par3 immunostaining was observed upon Par3b shRNA transduction in E12 cortical cells cultured for 3 days in vitro (see Fig. S1 in the supplementary material). Next we transduced cells isolated from E12 cortices in vitro with a low titer of each Par3 shRNA construct (shPar3a, b, c) or control plasmids. This allowed us to detect the transduced cells and/or their progeny by GFP fluorescence in individual clusters, i.e. the progeny derived from a single cell – a clone. Both the number of cells per clone and the proportion of neurons within clones were affected after transduction with Par3 shRNAs, in comparison to control, after 7 days in vitro (Fig. 2A-F). Par3a proved to be most efficient in reducing the mean clone size (to 24% of that of the control), whereas Par3c, the shRNA previously shown to be effective (Plusa et al., 2005), reduced the mean clone size to about half (56%) the size observed upon control transduction (Fig. 2F). It is noteworthy that the mean clone size obtained with the Par3a shRNA was close to the maximum achievable reduction, as virtually every clone ($84.5 \pm 13.5\%$ of all clones) consisted of only a single cell, whereas this was the case for just $43 \pm 15\%$ of clones transduced with control virus. The relatively high proportion of single-cell clones amongst control-infected cells was due to the use of lentiviral vectors that transduce postmitotic neurons as well as proliferating cells present at the beginning of the cultures. In addition, all Par3 shRNA constructs significantly reduced the number of clones that contained three or more cells (Fig. 2E). Examination of the cell fate after control transduction or Par3 knockdown revealed a significant increase, as compared with controls, in the proportion of transduced cells differentiating into neurons within the culture period (Fig. 2G). These results therefore suggest that knockdown of Par3 by three independent shRNAs potentially reduced clone size and drove many more cells towards a neuronal fate.

Time-lapse video microscopy reveals increased cell cycle exit upon Par3 knockdown

Our observations following Par3 knockdown using shRNA constructs could reflect increased exit from the cell cycle or cell death. To discriminate between these possibilities, we performed live time-lapse video microscopy of control and Par3b shRNA-transduced E12 cortical cells in vitro. We chose Par3b shRNA for these experiments, because it significantly decreased the number of cells per clone, but still allowed some cell divisions to occur (Fig. 2E). Transduced cells were identified by GFP fluorescence and their behavior was followed in phase-contrast images taken every 2 minutes during the culture period (see Materials and methods). The GFP fluorescence signal was first detected 2-3 days after lentiviral infection (see Movies 1, 2 in the supplementary material). At this time, we observed about $23 \pm 6\%$ of control-transduced cells as single cells. These cells were present as single cells from the beginning of the time-lapse imaging, and proved to be postmitotic neurons by subsequent immunolabeling for the neuronal marker MAP2 (also

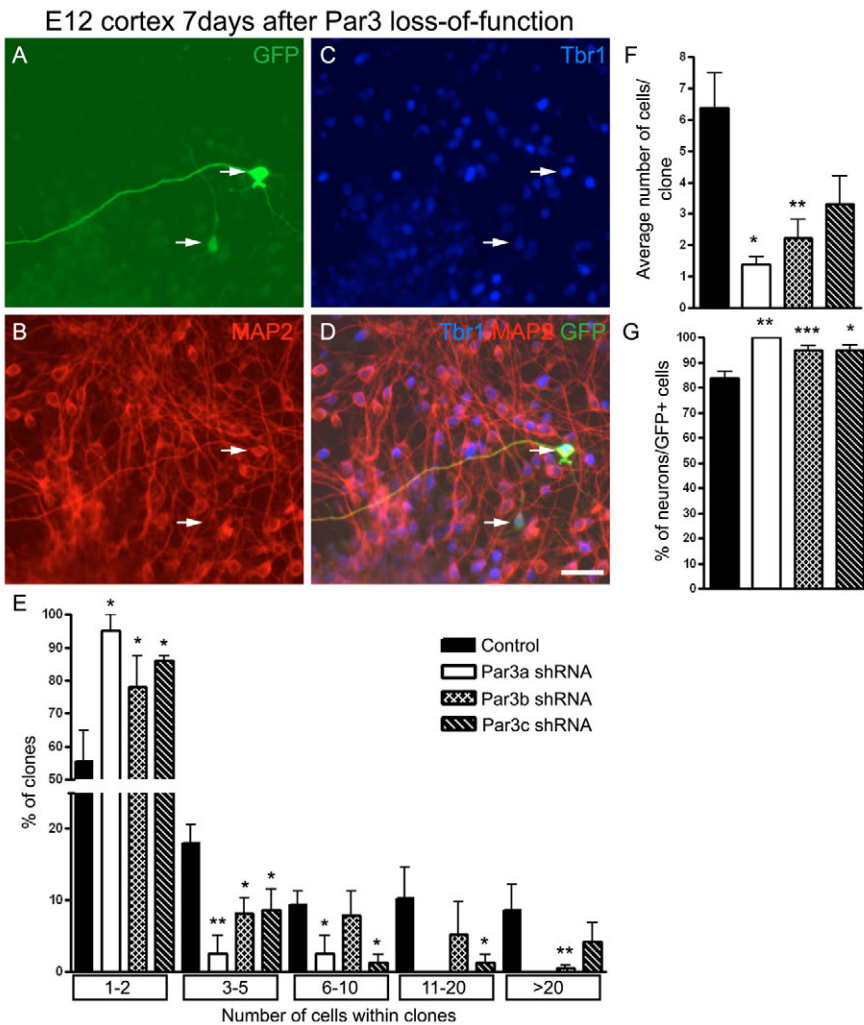


Fig. 2. Decreased proliferation of cortical progenitors after Par3 knockdown.

(A-D) Fluorescence micrographs depicting a two-cell clone generated from an E12 mouse cortical progenitor after Par3 shRNA transduction, immunolabeled for GFP (green), MAP2 (red) and Tbr1 (blue). Note that both GFP-positive cells express the neuronal markers MAP2 or Tbr1 (arrows). (E) Bar chart representing the frequency of control and Par3b shRNA-transduced cell clones according to the size (number of cells per clone, x-axis). Asterisks indicate statistically significant differences between control ($n=80$ clones) and Par3 shRNAs (Par3a, $n=40$; Par3b, $n=87$; Par3c, $n=57$ clones) for each clone size (*, $P<0.05$; **, $P<0.01$; Tukey's multiple comparison test). Note the lack of clones larger than 10 cells after Par3a shRNA-transduction. (F,G) Quantification of the mean number of GFP-positive cells per clone (F) and the proportion of neurons (G) generated after control or Par3 shRNA transduction (*, $P<0.05$; **, $P<0.01$; ***, $P<0.001$; Tukey's multiple comparison test). Scale bar: 25 μm .

known as Mtap2 – Mouse Genome Informatics) (data not shown). Apart from these postmitotic neurons, most cells in the control-infected cultures belonged to clones that were shown to derive from single progenitors undergoing one or more rounds of cell division (see Movie 1 in the supplementary material). By contrast, cells transduced with Par3b shRNA were mostly found as single cells ($77\pm 20\%$). None of these cells ever divided (46 cases analyzed). Thus, a significantly higher proportion of Par3b-transduced cells leaves the cell cycle and differentiates into neurons (see Movie 2 and Fig. S2 in the supplementary material). Moreover, those clones generated by Par3 shRNA-transduced cells that did contain a few more cells were usually small (2-6 cells) and the cell divisions took place during the first 2 days in vitro, with virtually all cells differentiating into neurons, as previously indicated in our clonal analysis (Fig. 2). Taken together, Par3 loss-of-function inhibits cell proliferation in cultured cortical progenitors, leading to premature cell cycle exit and neuronal differentiation.

Par3 knockdown in vivo interferes with the continuation of neurogenesis

Next, we transduced VZ progenitors in vivo by injecting control and Par3b shRNA-containing lentiviral vectors into the lateral ventricle of E12 embryos in utero (see Materials and methods for further details). First, we examined the location of GFP-labeled cells within the cortex 6 days after transduction, at E18 (Fig. 3A-

F). Most control- and Par3b shRNA-transduced cells had left the proliferating layers (VZ and SVZ) and migrated into the cortical plate (CP) (Fig. 3A-F). Interestingly, we noted that most control-transduced GFP-positive cells (60%) had already migrated into the upper part of the CP, the anlage of the upper cortical layers (Fig. 3A,B,G), whereas the majority of Par3b shRNA-transduced cells were contained in the deeper part of the CP (Fig. 3C,D,G). Virtually every Par3 shRNA-transduced neuron found in the deep cortical layers at E18 expressed Tbr1, a marker for deep-layer neurons (Fig. 3H,I), indicating that these cells have truly adopted a deep-layer fate. Moreover, Par3b shRNA-transduced cells were usually found as single cells (Fig. 3C,D,H), whereas control GFP-positive cells were often observed in groups of 2-4 cells (Fig. 3A,B). Taken together, these data suggest that most of the progenitors transduced with Par3 shRNA left the cell cycle shortly after infection at E12 and hence differentiated in most cases (70%, Fig. 3G) into deep-layer neurons. Taken together with the in vitro data, this suggests that Par3 is required to maintain cortical progenitor cells in a proliferative state and inhibit their neuronal differentiation.

Par3 and Par6 overexpression in vitro

To examine whether Par3 gain-of-function might have the opposite effect to the Par3 shRNA-mediated effects, we transduced E12 cortical progenitors with the full-length Par3 (180 kDa form, see

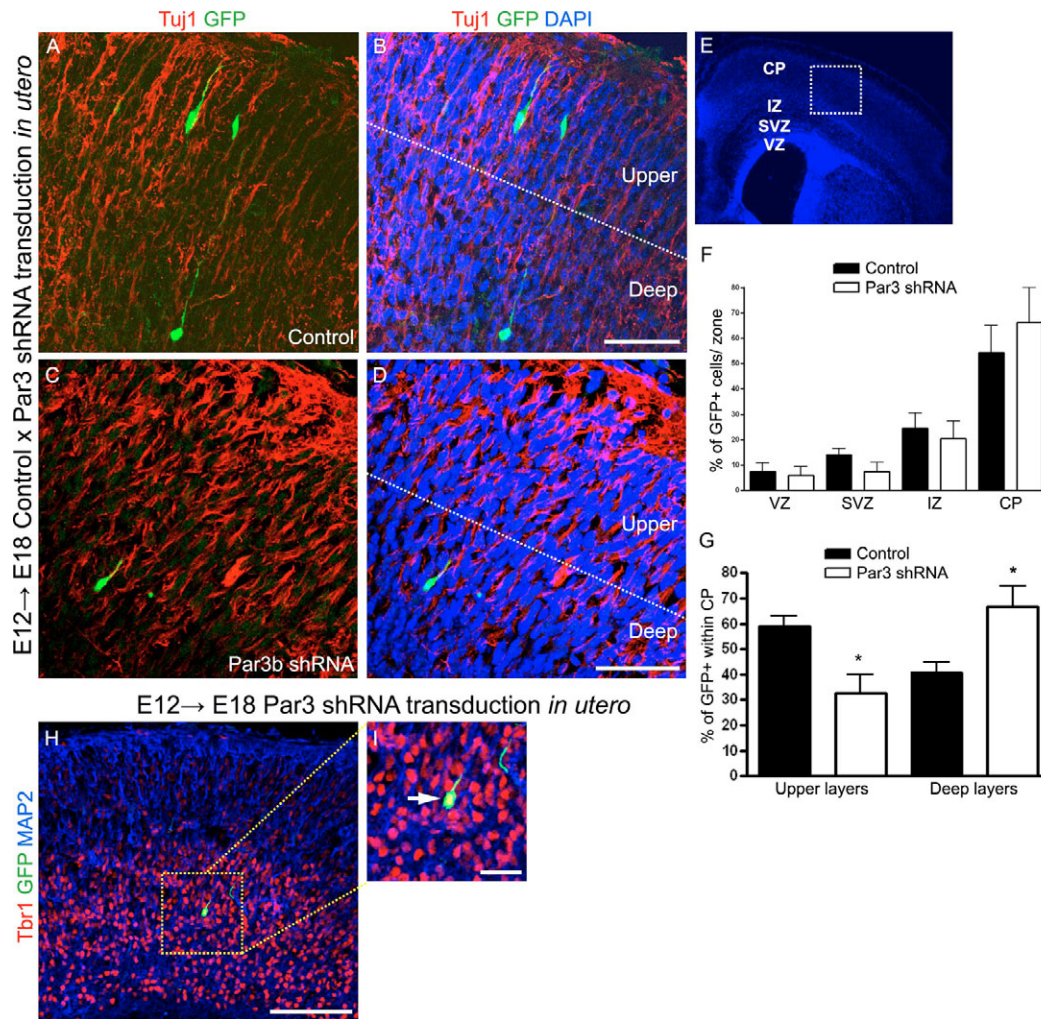


Fig. 3. Par3 loss-of-function increases the number of deep-layer neurons in vivo. (A-E) Fluorescence micrographs of E18 cortices injected with control (A,B) and Par3b shRNA (C,D) (6 days after injection) immunolabeled for GFP (green) and MAP2 (red) and stained with DAPI (blue). Note the GFP-positive neurons in both upper and deep cortical layers of a control-injected mouse (A,B). By contrast, a single GFP-positive neuron is found in the deep layers of a Par3b shRNA-injected mouse (C,D). (E) Representative section of E18 cortex indicating the different layers analyzed (VZ, SVZ, IZ and CP). (F,G) Histograms representing the proportion of GFP-positive cells in the cortex layers depicted in E (F) and GFP-positive neurons in the upper and deep cortical plate (G) of both control ($n=3$, 554 cells) and Par3b shRNA ($n=3$, 318 cells) -injected brains. Note the significant increase in neurons in the deep layers after Par3b shRNA transduction in comparison to the control (*, $P<0.05$; unpaired t -test). (H,I) Par3b shRNA-transduced neuron (arrow) colabeled for GFP (green), MAP2 (blue) and Tbr1 (red). VZ, ventricular zone; SVZ, subventricular zone; IZ, intermediate zone; CP, cortical plate. Scale bars: 40 μm in A,B; 50 μm in C,D; 100 μm in H; 25 μm in I.

Materials and methods for details) coexpressed with IRES GFP or a GFP-containing control retroviral vector. These viral vectors require breakdown of the nuclear envelope for viral genome integration and hence incorporate their genome only in proliferating cells (Price and Thurlow, 1988). As such, postmitotic neurons do not integrate these viral vectors, resulting in a smaller proportion of clones containing 1-2 cells than with the control lentivirus (compare controls in Figs 2, 4). Notably, transduction with Par3-containing retrovirus resulted in a significant increase (150%) in the mean size of clones in comparison to control-transduced clones after 7 days in vitro (Fig. 4A-F). This increase in clone size by Par3 transduction was mostly due to an increase in the number of large clones, containing more than 20 cells (Fig. 4E). Moreover, Par3-transduced cells comprised fewer neurons (Fig. 4G), indicating that a higher proportion of Par3-transduced cells (about 60%, Fig. 4G) maintained an undifferentiated state in comparison to controls (35%, Fig. 4G).

Taken together, Par3-transduced cells exhibit the opposite effect in clone size (an increase) to those subject to Par3 knockdown (a decrease).

We next examined whether Par6, another Par protein in the Par complex linking Par3 and aPKC to Cdc42 (Joberty et al., 2000), might have similar effects upon overexpression in cortical progenitors. Indeed, Par6 transduction resulted in a significant increase in the clone size 7 days after transduction of cells derived from both E12 (Fig. 5A,B) and E14 cortices (Fig. 5D,E). As observed for Par3-transduced cells, the increase in clone size upon Par6 transduction was mostly due to an increased proportion of clones containing more than 10 cells (Fig. 5A,D), and the proportion of neurons originating from E12 cortical progenitors was also reduced (Fig. 5C). Consistent with the hypothesized role of the Par complex in cell proliferation/differentiation and the diminished levels of Par proteins at mid-neurogenesis (Fig. 1), E14 progenitors

produced smaller clones than E12 progenitors (compare the controls in Fig. 5A,B and D,E), and the proportion of neurons between E14 control and Par6 clones was not affected (Fig. 5F). However, after Par6 overexpression, E14 cortical progenitors generated clones similar in size to those derived from E12 progenitors (Fig. 5B,E), indicating that the activation of the Par complex at later developmental stages is sufficient to promote proliferation.

Par6 overexpression in vitro increases symmetric progenitor cell division

To gain better insight into how Par6 mediates its potent role in promoting proliferation, we imaged live cell divisions by time-lapse video microscopy (see Movie 3 in the supplementary material). As described above, we tracked GFP-positive cells in phase-contrast images and determined their entire lineage tree over a culture period of 5 days. This allowed us to measure the cell cycle length for each cell division (see Fig. S3 in the supplementary material) and determine the fate of daughter cells at each cell division (Fig. 6). Based on daughter cell fate (dividing considered progenitors; non-dividing and later MAP2-immunopositive considered neurons) each cell division was classified as: (1) symmetric terminal (ST), when both daughter cells did not divide until the end of the movie (Fig. 6A, black stars); (2) asymmetric (As), when one of the daughter cells divided and the second did not (Fig. 6B,D, red stars); or (3) symmetric progenitor (SP), when both daughter cells divided again (Fig. 6C, green stars). All these modes of cell division were observed

in both control and Par6-transduced cultures (Fig. 6A-G). However, from the first to the fourth round of cell division, the frequency of SP divisions was significantly higher in the Par6-transduced cells than in the control (Fig. 6E-H). This increase largely occurred at the expense of ST cell divisions. In addition, the proportion of As cell divisions decreased in the Par6-transduced cells. In contrast to the pronounced changes in the mode of cell division, no difference was observed in the cell cycle length, either at the first, second, or third division of control and Par6-transduced cells (see Fig. S3 in the supplementary material). Thus, the increased number of proliferating cells detected after Par6 overexpression is caused by an increased frequency of symmetric divisions producing two progenitor cells.

Par6 overexpression in vitro increases the proportion of Pax6-expressing progenitors

To further examine the molecular identity of the progenitor cells generated upon Par6 overexpression, we analyzed pairs of cells 2 days after transduction in vitro (Shen et al., 2002; Kawaguchi et al., 2004; Clayton et al., 2007). We used low numbers of viral particles in order to obtain a small number of pairs that could thereby be inferred as being derived from a single progenitor. First, we examined progenitor identity by staining for Ki67. Consistent with the time-lapse analysis, the number of pairs with both cells expressing Ki67 was significantly increased, in comparison to the control, after Par6 overexpression (see Fig. S4 in the supplementary

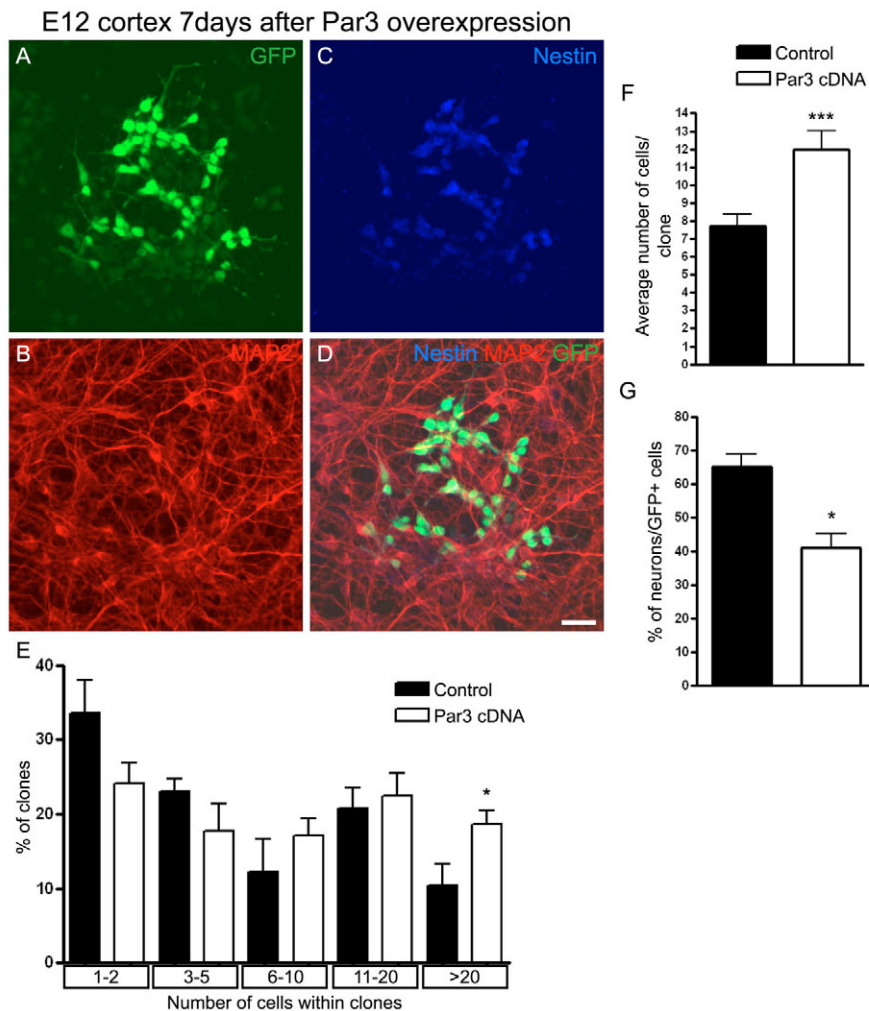


Fig. 4. Increased clone size upon overexpression of mouse Par3 in vitro. (A-D) GFP-labeled clone in E12 cortex dissociated-cell cultures after Par3 transduction and 7-days culture. Immunolabeled for GFP (A and D, green), nestin (C and D, blue) and MAP2 (B and D, red). Note the high number of nestin-positive MAP2-negative cells. (E-G) Bar charts representing the size (E,F) and neuronal content (G) of clones generated from E12 cortical cells after transduction with control or Par3-containing retroviral vectors. Note the significant increase in the average clone size (F; ***, $P < 0.001$; unpaired t -test), as well as in the frequency of clones containing 20 or more cells (E; *, $P < 0.05$; unpaired t -test) after Par3 transduction ($n = 132$) in comparison to the control ($n = 170$). The proportion of neurons amongst GFP+ transduced cells was also significantly reduced after Par3 gain-of-function (G; **, $P < 0.01$; unpaired t -test). Scale bar: 50 μm .

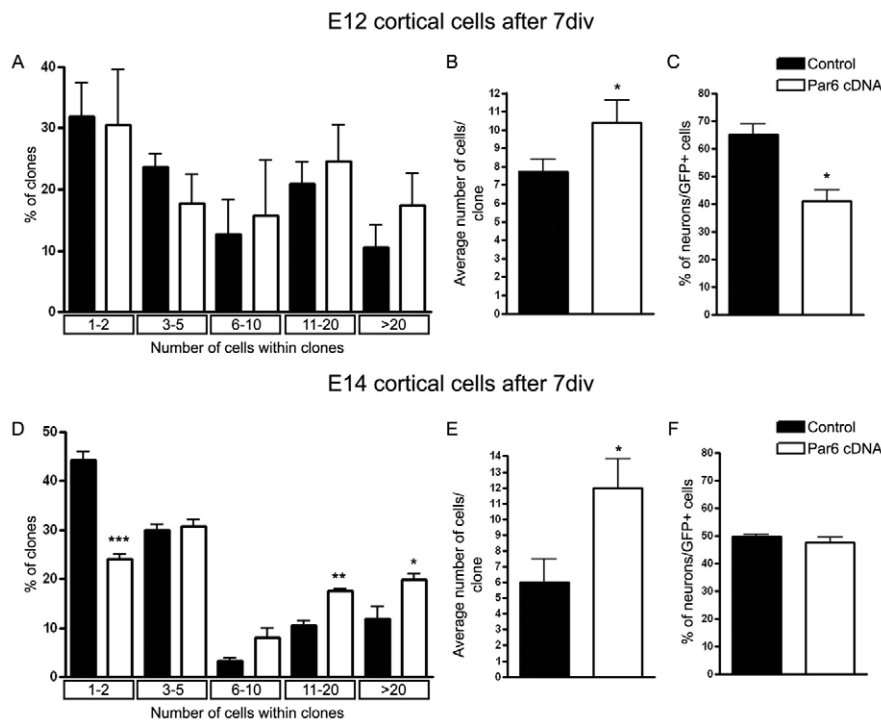


Fig. 5. Increased clone size upon overexpression of mouse Par6 in vitro. (A-F) Bar charts representing the composition of clones generated from E12 (A-C) or E14 (D-F) cortical cells transduced with either control or Par6-containing plasmids after 7 days in vitro (7div). Par6 overexpression increased the mean number of cells per clone (A and D; *, $P < 0.05$; unpaired t -test) as well as the frequency of large clones (C and F; *, $P < 0.05$; unpaired t -test) in both E12 (control, $n = 150$; Par6, $n = 150$) and E14 (control, $n = 80$; Par6, $n = 96$) cell cultures, with a stronger effect in the E14 cells (compare A-C and D-F). The proportion of neurons within clones was also significantly reduced in both sets of experiments (B and D; *, $P < 0.05$; unpaired t -test).

material). Thus, the pair analysis provided a reliable read-out of cell divisions as observed by time-lapse video microscopy. Next, we examined the molecular identity of the progenitors by staining for Pax6, a transcription factor expressed in virtually all self-renewing VZ cells (Götz et al., 1998; Englund et al., 2005; Cappello et al., 2006), versus Tbr2, a transcription factor expressed in the basal SVZ progenitor cells (Englund et al., 2005; Cappello et al., 2006). Strikingly, whereas the frequency of Pax6-positive pairs significantly increased after Par6 overexpression (Fig. 7A-J; $P < 0.01$, unpaired t -test), the frequency of Tbr2-positive pairs was not, and the proportion of pairs with both daughters expressing Tbr2 was higher (by almost double) in the control-transduced cells (Fig. 7K; $P < 0.01$, unpaired t -test). These data demonstrate for the first time that the Par complex is upstream of these fate determinants, demonstrating that Par6 overexpression is sufficient to maintain progenitors in a Pax6-expressing self-renewing state.

Par6 overexpression in vivo increases the proportion of Pax6-positive VZ progenitors

In the final set of experiments, we examined whether Par6 overexpression would similarly promote Pax6-positive VZ progenitor fate in vivo. Retroviral vectors were injected into the lateral ventricle of E13 mice and embryos analyzed 3 days later. At E16, we observed a striking increase in the number of GFP-positive cells in Par6-injected brains in comparison with the control (Fig. 8A,B). This effect was consistently reproduced in littermates infected with the same number of viral particles, consistent with the in vitro observation that Par6 overexpression increased the number of labeled cells, presumably by promoting cell proliferation. Indeed, the proportion of Par6-transduced GFP-positive cells within the VZ increased to more than double that observed in control-infected cells (Fig. 8C). By contrast, the proportion of GFP-positive cells in the SVZ was not altered upon Par6 transduction (Fig. 8C). An increase in the proportion of cells in the VZ may be due to a failure of these cells to migrate radially, as previously described in the cerebellum upon manipulation of Par6 (Solecki et al., 2004), and/or to the

maintenance of a progenitor state by Par6 overexpression. In support of the latter, double staining for GFP and Ki67 showed that the vast majority of GFP-positive cells in the VZ of Par6-injected mice were colabeled (Fig. 8D), supporting their progenitor-cell identity. Moreover, in virtually every case, Par6-transduced VZ cells also double labeled with the VZ progenitor marker Pax6 (Fig. 8E). At SVZ positions, some cells also contained Tbr2 (Fig. 8F), but the proportion of such cells was not increased upon Par6 overexpression (Fig. 8C). Moreover, neither VZ nor SVZ cells transduced with Par6 contained the neuron-specific antigen MAP2 (Fig. 8G), consistent with their progenitor fate. Taken together, Par6 overexpression promotes the maintenance of Pax6-positive VZ progenitors both in vitro and in vivo.

DISCUSSION

In this work, we provide several lines of evidence that the Par complex controls proliferative VZ progenitor fate in the developing mouse cortex. Consistent with our immunohistochemical data showing a decrease in the endogenous levels of Par-complex proteins correlating with a decrease of the cortical progenitor pool, overexpression of Par proteins resulted in a notable increase in the number of proliferating VZ progenitors in vitro and in vivo. Live observation of lineage trees in vitro demonstrated that overexpression of Par6 selectively promoted symmetric proliferative cell divisions, while not affecting the cell cycle length. Knockdown of Par3 resulted in the opposite phenotype, thereby confirming the role of endogenous Par proteins in promoting proliferative cell divisions in vivo and in vitro.

Role of the Par complex in proliferation and the mode of cell division

Much of our knowledge on the function of polarity genes is derived from studies of *Drosophila* neuroblasts, which give rise to two daughter cells of distinct size and fate. The smaller basal daughter cell (ganglion mother cell, GMC) undergoes terminal division to generate two neurons or glia, whereas the larger apical daughter

maintains a neuroblast identity and continues to divide, generating new neuroblasts and GMCs (reviewed by Betschinger and Knoblich, 2004). The molecular mechanisms controlling the specification of these two types of cells have been extensively studied and are reviewed elsewhere (e.g. Betschinger and Knoblich, 2004; Yu et al., 2006). Particularly relevant for our results, the Par-complex proteins Bazooka (the fly homolog of Par3), Par6 and aPKC have been shown to localize apically in the neuroblasts and to be inherited by the large apical daughter cell, which continues to

divide in a stem-cell-like fashion. Our results indicate similarities and differences in the role of Par-complex proteins in the mouse cerebral cortex. Par3 and Par6 also play an important role in the control of proliferation and differentiation, but they differ with regard to their effects on asymmetric cell division. Overexpression of Par6 did not significantly affect the number of asymmetric cell divisions. If asymmetric distribution of Par6 was required for asymmetric cell division, overexpression of Par6 should result in inheritance by both daughter cells and hence should abolish

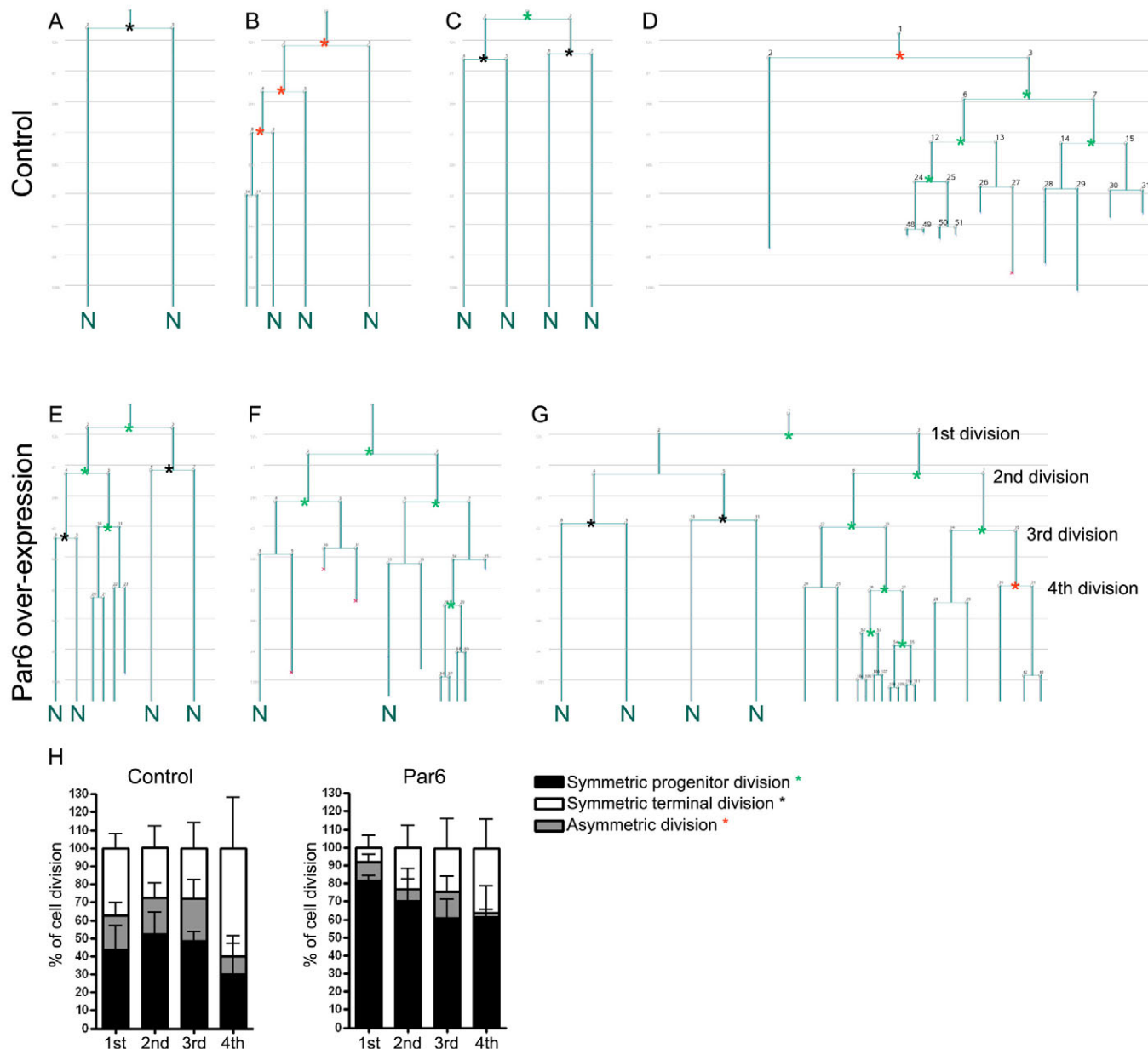


Fig. 6. Lineage analysis by time-lapse video microscopy of control and Par6-transduced progenitors. (A-G) Examples of lineage trees from control (A-D) and Par6-transduced (E-G) cells obtained from time-lapse images taken every 2 minutes over a period of 5 days. Horizontal grid lines indicate every 12 hours of the experiment. Colored stars indicate cell divisions generating two progenitors (green), two postmitotic cells (black) or one progenitor and one postmitotic cell (red). Most cells leaving the cell cycle more than 36 hours before the end of the movies were identified in subsequent immunolabelings as MAP2-positive neurons (N) (see also Fig. S2 in the supplementary material). Horizontal lines indicate the time point of cell division. The length of the horizontal line is arbitrary and has no significance. The lengths of the vertical lines depicts the time elapsed between two cell divisions, i.e. the cell cycle length. (H) Quantification of symmetric progenitor, symmetric terminal and asymmetric cell divisions in the first, second, third and fourth cell divisions. Note the higher frequency of symmetric progenitor cell divisions in the lineages derived from Par6-transduced cells ($n=56$) in comparison to controls ($n=68$).

asymmetric cell divisions. Indeed, it has been shown that ectopic expression of Par3 is sufficient to mislocalize the entire Par complex in transduced neuroepithelial cells in chicken embryos (Afonso and Henrique, 2006). As neither Par3 nor Par6 overexpression abolished asymmetric cell divisions in cortical progenitors, it appears that the role of Par3 and Par6 in regulating proliferation in the mouse cerebral cortex may be independent of asymmetric cell division and/or the asymmetric inheritance of the Par protein itself.

Consistent with profound differences in the mode of Par-complex function between *Drosophila* and vertebrates, little effect on spindle orientation has been observed after Par3 manipulation in the zebrafish neuroepithelium (von Trotha et al., 2006) (but see Horne-Badovinac et al., 2001), whereas defects in Par-complex-mediated

signaling affect spindle orientation in *Drosophila* (Kuchinke et al., 1998; Wodarz et al., 2000; Petronczki and Knoblich, 2001). Indeed, a major difference between vertebrate and invertebrate neurogenesis appears to be the mode of cell division. Only a minority of neural

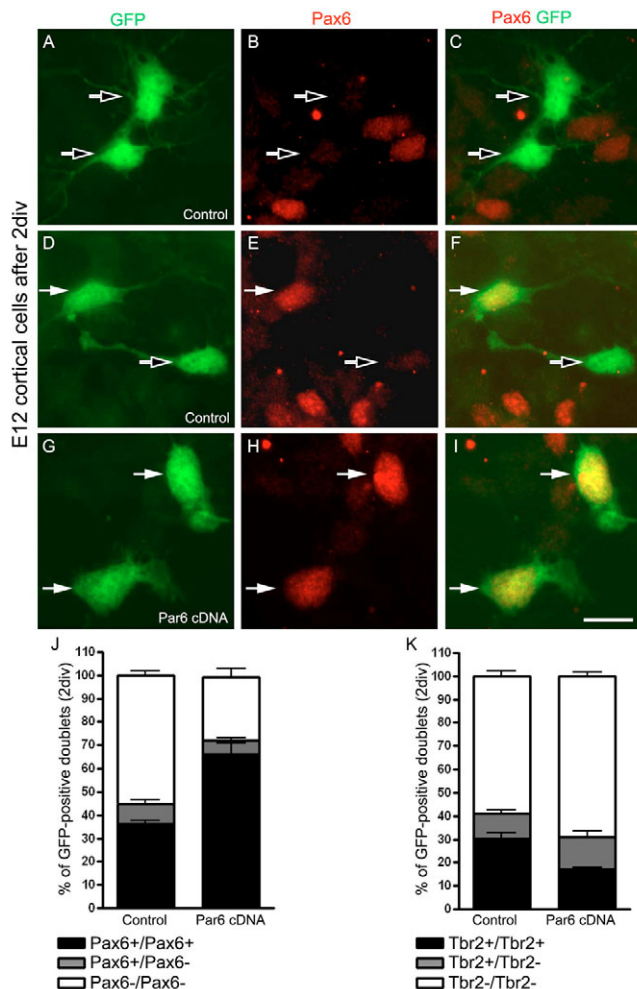


Fig. 7. Par6 overexpression increases the number of Pax6+ progenitors. (A-I) Examples of two-cell clones (pairs) obtained from E12 mouse cortical cells transduced with control (A-F) or Par6 (G-I) cDNA and immunolabeled for GFP (green) and Pax6 (red) after 2 days in vitro (2div). White arrows point to Pax6/GFP double-positive cells and black arrows to GFP-positive Pax6 negative cells. (J) Bar chart depicting the frequency of pairs (control, $n=84$; Par6, $n=59$) containing two Pax6-positive cells (black bar), only one Pax6-positive cell (gray), or only Pax6-negative cells (white). (K) Bar chart representing the same quantification as in J but for Tbr2 (control, $n=61$; Par6, $n=54$). Note the increased proportion of pairs containing two Pax6-positive cells after Par6 overexpression. By contrast, the frequency of pairs containing two Tbr2-positive cells was significantly reduced after Par6 transduction. Scale bar: 25 μm .

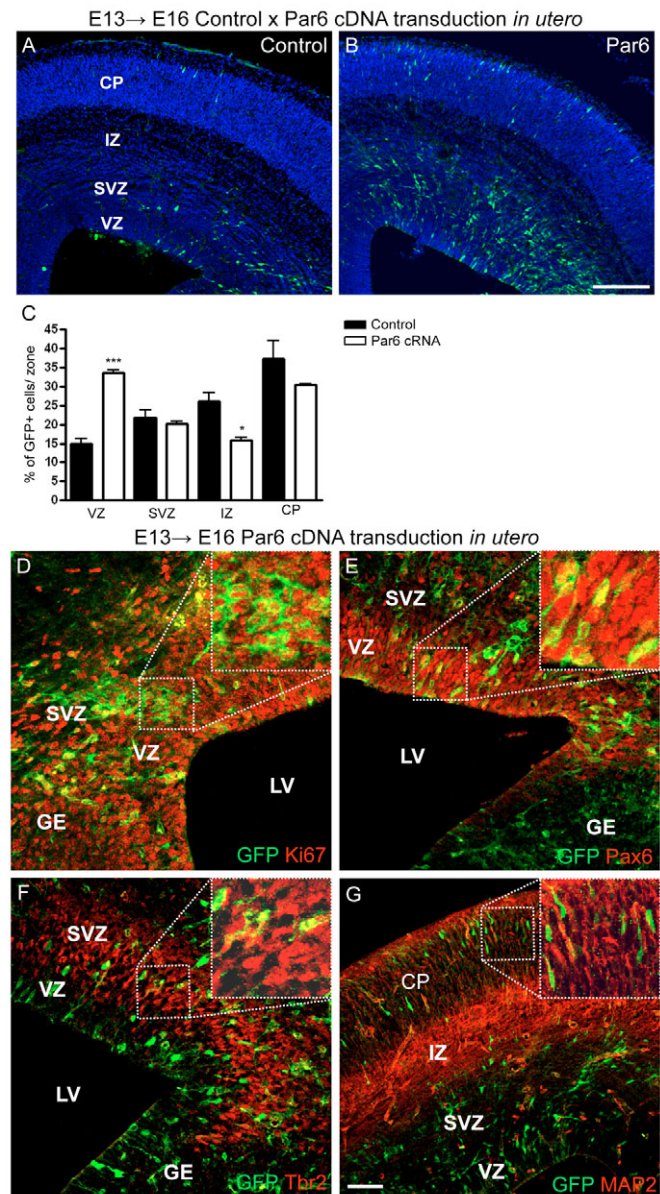


Fig. 8. Par6 overexpression in vivo increases the number of Pax6+ VZ progenitors. (A,B) Coronal sections of E16 cerebral cortices injected with either control (A) or Par6-containing (B) retroviruses at E13, immunolabeled for GFP (green) and stained with DAPI (blue). (C) Quantification of GFP-positive cells in the dorsal telencephalon of control ($n=4$, 1642 cells) and Par6 ($n=3$, 3568 cells)-injected brains. Note the increased proportion of GFP-positive cells in the VZ of Par6-injected animals (***, $P<0.001$; unpaired t -test), whereas the proportion of GFP-positive cells in the cortical plate and intermediate zone was reduced (*, $P<0.05$; unpaired t -test). (D-G) Higher-power micrographs of coronal sections of E16 cortices injected with Par6-containing retroviruses and double labeled as indicated. Insets are higher magnifications of the boxed areas. VZ, ventricular zone; SVZ, subventricular zone; IZ, intermediate zone; CP, cortical plate; LV, lateral ventricle; GE, ganglionic eminences. Scale bars: 100 μm in A,B; 50 μm in D-F; 75 μm in G.

progenitors divide obliquely to the apico-basal axis in vertebrate neuroepithelia (Lyons et al., 2003; Götz and Huttnner, 2005; Das et al., 2003; Kosodo et al., 2004; Stricker et al., 2006), in contrast to the predominant asymmetric mode of cell division of *Drosophila* neuroblasts (for a review, see Yu et al., 2006). Asymmetry in daughter cell fate also occurs in the vertebrate nervous system, but whether or not this is achieved by the asymmetric inheritance of fate determinants (Kosodo et al., 2004), extrinsic signals or yet unresolved mechanisms, is still not clear.

Importantly, the characteristically low proportion of asymmetric cell divisions in the mammalian cortex also persists *in vitro* – in slice cultures (Miyata et al., 2004), single-cell cultures (Qian et al., 1998) and in our high-density dissociated cortical cultures. Live imaging in cortical slice cultures demonstrated that in most cases (73%) apical VZ progenitors divide symmetrically to generate two progenitors, and in only 27% of cases asymmetrically (Miyata et al., 2004). In addition to these VZ progenitors, about 30% of all progenitors at this stage are basal SVZ progenitors that divide in a terminally symmetric cell division (Haubst et al., 2004; Cappello et al., 2006; Noctor et al., 2004; Miyata et al., 2004; Haubensak et al., 2004). Therefore, amongst all progenitor cells, a third divides in a terminally symmetric manner (all SVZ cells), half divide in a proliferative symmetric manner (70% of all VZ cells), and only 20% (30% of VZ cells) divide in an asymmetric manner. These proportions are strikingly similar to those observed in our time-lapse analysis.

The similarity in the effect of Par protein manipulations *in vivo* and in dissociated-cell cultures in our study implies that tissue polarity and coordinated apico-basal fate determinants are not required for the Par complex to influence cell proliferation. As cell polarity is not required for the Par complex to exert its effect, and as asymmetric cell divisions were not abolished by Par6 overexpression, we suggest that the overall level and activity of the Par complex might determine cell proliferation in a threshold manner. Interestingly, the apically located Par complex is mostly symmetrically distributed in the zebrafish neuroepithelium (von Trotha et al., 2006; Tawk et al., 2007), where it is required for the mirror-symmetric cell divisions that occur during neural keel formation (Tawk et al., 2007), as well as in the mouse VZ (Kosodo et al., 2004). A unifying model might therefore be one in which the amount of apically located Par protein determines whether both cells continue to proliferate (high levels of Par protein, as upon overexpression or early in development), or only one cell continues to proliferate (stochastically, upon lower Par protein levels), or no cells continue to proliferate (as observed after Par3 knockdown or at the end of neurogenesis). This model not only fits very well with the results obtained by our manipulation of Par protein levels, but also with our observation that the Par proteins decrease considerably at the apical surface during cortical development, thereby causing the reduction in the progenitor pool. Moreover, the low level of Par proteins around mid-neurogenesis in apical progenitors explains the mild phenotype upon deletion of aPKC λ or Cdc42 at these later stages (Cappello et al., 2006; Imai et al., 2006), in contrast to the much stronger effects upon their deletion at earlier stages (Cappello et al., 2006). Taken together, these results suggest a role of the Par complex in proliferation that appears to be rather independent on an asymmetric distribution of Par3 and Par6, but which also employs Cdc42 and aPKC (Rolls et al., 2003; Castoria et al., 2004; Imai et al., 2006; Cappello et al., 2006).

Role of the Par complex in cell-fate specification

One of the most striking results obtained by the manipulation of Par proteins in our study is their instruction of a specific type of progenitor, namely the Pax6-positive VZ progenitors. Par3 and

Par6 overexpression promote progenitors that express Pax6 and not Tbr2. Whereas VZ progenitors that contain different levels of Pax6 proliferate to different degrees, the basal SVZ progenitors that are characterized by expression of a different set of transcription factors [Tbr2, Svet1, Cux2 (Cutl2), or Prox1] (Tarabykin et al., 2001; Nieto et al., 2004; Zimmer et al., 2004; Englund et al., 2005; Lavado and Oliver, 2007) most often generate two postmitotic daughters. Thus, overexpression of Par6 may exert its effect by instructing a VZ fate, an indicator of which is the expression of Pax6. However, deletion of Pax6 results in a greater number of progenitors (Haubst et al., 2004), suggesting that Pax6 itself is not mediating the proliferative function exerted by Par3 or Par6 overexpression. Indeed, overexpression of Pax6 rather promotes exit from the cell cycle (Quinn et al., 2007) and differentiation into neurons (Haubst et al., 2004; Hack et al., 2004; Heins et al., 2002). However, Pax6 is expressed at different levels in all VZ/radial glial cells and recent experiments have shown differences between Pax6 isoforms present in the self-renewing radial glia versus the radial glia that directly generate postmitotic neurons (L. Pinto and M.G., unpublished). Thus, the increased proportion of Pax6+ cells indicates an increase of progenitors with a radial glia/VZ fate, at the expense of SVZ progenitors (Tbr2+ cells). Interestingly, upper-layer neurons have been proposed to derive largely via basal SVZ progenitor cells (Tarabykin et al., 2001; Nieto et al., 2004; Zimmer et al., 2004; Schuurmans et al., 2004; Wu et al., 2005). This suggests that the maintenance of progenitors in the VZ fate, as achieved upon Par6 overexpression *in vivo*, might interfere with upper-layer neuron generation. Conversely, however, the knockdown of Par proteins does not increase the generation of upper-layer neurons, most likely because they exit from the cell cycle too prematurely. Our observation that the overexpression of Par-complex proteins promotes the fate of Pax6+ VZ progenitors is also consistent with the results obtained after deletion of Cdc42, the activator of the Par complex, upon which Pax6-positive self-renewing progenitors are lost and Tbr2-positive progenitors dividing in a differentiative mode are increased (Cappello et al., 2006). Notably, the reduction in Pax6 levels is very mild upon deletion of Cdc42 at later stages (Cappello et al., 2006) (data not shown), consistent with the reduced amount of Par proteins at this later stage. Interestingly, Par6 has recently been observed in the nucleus (Cline and Nelson, 2007), implying the possibility that Par proteins might indeed participate in the regulation of gene transcription. Thus, our data not only demonstrate the key role of Par proteins in regulating self-renewing progenitors, but also suggest a novel role for Par proteins in regulating the expression of transcriptional cell-fate determinants.

We thank Silvia Cappello for initial experiments with Par3 overexpression; Leanne Godinho and Marie-Theres Schmid for excellent comments on the manuscript; and Detlef Franzen, Angelika Waiser and Andrea Steiner-Mezzadri for expert technical help. The DFG, EU, BMBF and FORNEUROCELL (to M.G.) supported this work. M.R.C. was supported by an Alexander-von-Humboldt postdoctoral fellowship.

Supplementary material

Supplementary material for this article is available at <http://dev.biologists.org/cgi/content/full/135/1/11/DC1>

References

- Afonso, C. and Henrique, D. (2006). PAR3 acts as a molecular organizer to define the apical domain of chick neuroepithelial cells. *J. Cell Sci.* **119**, 4293–4304.
- Astrom, K. E. and Webster, H. D. (1991). The early development of the neopallial wall and area choroidea in fetal rats. A light and electron microscopic study. *Adv. Anat. Embryol. Cell Biol.* **123**, 1–76.

- Betschinger, J. and Knoblich, J. A.** (2004). Dare to be different: asymmetric cell division in *Drosophila*, *C. elegans* and vertebrates. *Curr. Biol.* **14**, R674-R685.
- Cappello, S., Attardo, A., Wu, X., Iwasato, T., Itohara, S., Wilsch-Brauninger, M., Eilken, H. M., Rieger, M. A., Schroeder, T. T., Huttner, W. B. et al.** (2006). The Rho-GTPase *cdc42* regulates neural progenitor fate at the apical surface. *Nat. Neurosci.* **9**, 1099-1107.
- Castoria, G., Migliaccio, A., Di Domenico, M., Lombardi, M., de Falco, A., Varricchio, L., Bilancio, A., Barone, M. V. and Auricchio, F.** (2004). Role of atypical protein kinase C in estradiol-triggered G1/S progression of MCF-7 cells. *Mol. Cell. Biol.* **24**, 7643-7653.
- Chenn, A. and McConnell, S. K.** (1995). Cleavage orientation and the asymmetric inheritance of Notch1 immunoreactivity in mammalian neurogenesis. *Cell* **82**, 631-641.
- Clayton, E., Doupe, D. P., Klein, A. M., Winton, D. J., Simons, B. D. and Jones, P. H.** (2007). A single type of progenitor cell maintains normal epidermis. *Nature* **446**, 185-189.
- Cline, E. G. and Nelson, W. J.** (2007). Characterization of Mammalian par 6 as a dual-location protein. *Mol. Cell. Biol.* **27**, 4431-4443.
- Das, T., Payer, B., Cayouette, M. and Harris, W. A.** (2003). In vivo time-lapse imaging of cell divisions during neurogenesis in the developing zebrafish retina. *Neuron* **37**, 597-609.
- Dehay, C. and Kennedy, H.** (2007). Cell-cycle control and cortical development. *Nat. Rev. Neurosci.* **8**, 438-450.
- Desai, A. R. and McConnell, S. K.** (2000). Progressive restriction in fate potential by neural progenitors during cerebral cortical development. *Development* **127**, 2863-2872.
- Englund, C., Fink, A., Lau, C., Pham, D., Daza, R. A., Bulfone, A., Kowalczyk, T. and Hevner, R. F.** (2005). Pax6, Tbr2, and Tbr1 are expressed sequentially by radial glia, intermediate progenitor cells, and postmitotic neurons in developing neocortex. *J. Neurosci.* **25**, 247-251.
- Götz, M. and Huttner, W. B.** (2005). The cell biology of neurogenesis. *Nat. Rev. Mol. Cell Biol.* **6**, 777-788.
- Götz, M., Stoykova, A. and Gruss, P.** (1998). Pax6 controls radial glia differentiation in the cerebral cortex. *Neuron* **21**, 1031-1044.
- Hack, M. A., Sugimori, M., Lundberg, C., Nakafuku, M. and Gotz, M.** (2004). Regionalization and fate specification in neurospheres: the role of Olig2 and Pax6. *Mol. Cell. Neurosci.* **25**, 664-678.
- Haubensak, W., Attardo, A., Denk, W. and Huttner, W. B.** (2004). Neurons arise in the basal neuroepithelium of the early mammalian telencephalon: a major site of neurogenesis. *Proc. Natl. Acad. Sci. USA* **101**, 3196-3201.
- Haubst, N., Berger, J., Radjendirane, V., Graw, J., Favor, J., Saunders, G. F., Stoykova, A. and Gotz, M.** (2004). Molecular dissection of Pax6 function: the specific roles of the paired domain and homeodomain in brain development. *Development* **131**, 6131-6140.
- Haydar, T. F., Ang, E., Jr and Rakic, P.** (2003). Mitotic spindle rotation and mode of cell division in the developing telencephalon. *Proc. Natl. Acad. Sci. USA* **100**, 2890-2895.
- Heins, N., Cremisi, F., Malatesta, P., Gangemi, R. M., Corte, G., Price, J., Goudreau, G., Gruss, P. and Gotz, M.** (2001). *Emx2* promotes symmetric cell divisions and a multipotential fate in precursors from the cerebral cortex. *Mol. Cell. Neurosci.* **18**, 485-502.
- Heins, N., Malatesta, P., Cecconi, F., Nakafuku, M., Tucker, K. L., Hack, M. A., Chapouton, P., Barde, Y. A. and Gotz, M.** (2002). Glial cells generate neurons: the role of the transcription factor Pax6. *Nat. Neurosci.* **5**, 308-315.
- Horne-Badovinac, S., Lin, D., Waldron, S., Schwarz, M., Mbamalu, G., Pawson, T., Jan, Y., Stainier, D. Y. and Abdellilah-Seyfried, S.** (2001). Positional cloning of heart and soul reveals multiple roles for PKC lambda in zebrafish organogenesis. *Curr. Biol.* **11**, 1492-1502.
- Imai, F., Hirai, S., Akimoto, K., Koyama, H., Miyata, T., Ogawa, M., Noguchi, S., Sasaoka, T., Noda, T. and Ohno, S.** (2006). Inactivation of aPKC lambda results in the loss of adherens junctions in neuroepithelial cells without affecting neurogenesis in mouse neocortex. *Development* **133**, 1735-1744.
- Joberty, G., Petersen, C., Gao, L. and Macara, I. G.** (2000). The cell-polarity protein Par6 links Par3 and atypical protein kinase C to Cdc42. *Nat. Cell Biol.* **2**, 531-539.
- Kawaguchi, A., Ogawa, M., Saito, K., Matsuzaki, F., Okano, H. and Miyata, T.** (2004). Differential expression of Pax6 and Ngn2 between pair-generated cortical neurons. *J. Neurosci. Res.* **78**, 784-795.
- Kosodo, Y., Roper, K., Haubensak, W., Marzesco, A. M., Corbeil, D. and Huttner, W. B.** (2004). Asymmetric distribution of the apical plasma membrane during neurogenic divisions of mammalian neuroepithelial cells. *EMBO J.* **23**, 2314-2324.
- Kovac, J., Oster, H. and Leitges, M.** (2007). Expression of the atypical protein kinase C (aPKC) isoforms *iota* and *lambda* and *zeta* during mouse embryogenesis. *Gene Expr. Patterns* **7**, 187-196.
- Kuchinke, U., Grawe, F. and Knust, E.** (1998). Control of spindle orientation in *Drosophila* by the Par-3-related PDZ-domain protein Bazooka. *Curr. Biol.* **8**, 1357-1365.
- Lavado, A. and Oliver, G.** (2007). Prox1 expression patterns in the developing and adult murine brain. *Dev. Dyn.* **236**, 518-524.
- Lukaszewicz, A., Savatier, P., Cortay, V., Giroud, P., Huissoud, C., Berland, M., Kennedy, H. and Dehay, C.** (2005). G1 phase regulation, area-specific cell cycle control, and cytoarchitectonics in the primate cortex. *Neuron* **47**, 353-364.
- Lyons, D. A., Guy, A. T. and Clarke, J. D.** (2003). Monitoring neural progenitor fate through multiple rounds of division in an intact vertebrate brain. *Development* **130**, 3427-3436.
- Manabe, N., Hirai, S., Imai, F., Nakanishi, H., Takai, Y. and Ohno, S.** (2002). Association of ASIP/mPAR-3 with adherens junctions of mouse neuroepithelial cells. *Dev. Dyn.* **225**, 61-69.
- Miyata, T., Kawaguchi, A., Okano, H. and Ogawa, M.** (2001). Asymmetric inheritance of radial glial fibers by cortical neurons. *Neuron* **31**, 727-741.
- Miyata, T., Kawaguchi, A., Saito, K., Kawano, M., Muto, T. and Ogawa, M.** (2004). Asymmetric production of surface-dividing and non-surface-dividing cortical progenitor cells. *Development* **131**, 3133-3145.
- Mizuguchi, R., Sugimori, M., Takebayashi, H., Kosako, H., Nagao, M., Yoshida, S., Nabeshima, Y., Shimamura, K. and Nakafuku, M.** (2001). Combinatorial roles of *olig2* and *neurogenin2* in the coordinated induction of pan-neuronal and subtype-specific properties of motoneurons. *Neuron* **31**, 757-771.
- Mollgard, K., Balslev, Y., Lauritzen, B. and Saunders, N. R.** (1987). Cell junctions and membrane specializations in the ventricular zone (germinal matrix) of the developing sheep brain: a CSF-brain barrier. *J. Neurocytol.* **16**, 433-444.
- Nieto, M., Monuki, E. S., Tang, H., Imitola, J., Haubst, N., Khoury, S. J., Cunningham, J., Gotz, M. and Walsh, C. A.** (2004). Expression of *Cux-1* and *Cux-2* in the subventricular zone and upper layers II-IV of the cerebral cortex. *J. Comp. Neurol.* **479**, 168-180.
- Noctor, S. C., Flint, A. C., Weissman, T. A., Dammerman, R. S. and Kriegstein, A. R.** (2001). Neurons derived from radial glial cells establish radial units in neocortex. *Nature* **409**, 714-720.
- Noctor, S. C., Martinez-Cerdeno, V., Ivic, L. and Kriegstein, A. R.** (2004). Cortical neurons arise in symmetric and asymmetric division zones and migrate through specific phases. *Nat. Neurosci.* **7**, 136-144.
- Petronczki, M. and Knoblich, J. A.** (2001). DmPAR-6 directs epithelial polarity and asymmetric cell division of neuroblasts in *Drosophila*. *Nat. Cell Biol.* **3**, 43-49.
- Plusa, B., Frankenberg, S., Chalmers, A., Hadjantonakis, A. K., Moore, C. A., Papalopulu, N., Papaioannou, V. E., Glover, D. M. and Zernicka-Goetz, M.** (2005). Downregulation of Par3 and aPKC function directs cells towards the ICM in the preimplantation mouse embryo. *J. Cell Sci.* **118**, 505-515.
- Price, J. and Thurlow, L.** (1988). Cell lineage in the rat cerebral cortex: a study using retroviral-mediated gene transfer. *Development* **104**, 473-482.
- Qian, X., Goderie, S. K., Shen, Q., Stern, J. H. and Temple, S.** (1998). Intrinsic programs of patterned cell lineages in isolated vertebrate CNS ventricular zone cells. *Development* **125**, 3143-3152.
- Quinn, J. C., Molinek, M., Martynoga, B. S., Zaki, P. A., Faedo, A., Bulfone, A., Hevner, R. F., West, J. D. and Price, D. J.** (2007). Pax6 controls cerebral cortical cell number by regulating exit from the cell cycle and specifies cortical cell identity by a cell autonomous mechanism. *Dev. Biol.* **302**, 50-65.
- Rakic, P.** (1988). Specification of cerebral cortical areas. *Science* **241**, 170-176.
- Rolls, M. M., Albertson, R., Shih, H. P., Lee, C. Y. and Doe, C. Q.** (2003). *Drosophila* aPKC regulates cell polarity and cell proliferation in neuroblasts and epithelia. *J. Cell Biol.* **163**, 1089-1098.
- Schuermans, C., Armant, O., Nieto, M., Stenman, J. M., Britz, O., Klenin, N., Brown, C., Langevin, L. M., Seibt, J., Tang, H. et al.** (2004). Sequential phases of cortical specification involve Neurogenin-dependent and -independent pathways. *EMBO J.* **23**, 2892-2902.
- Shen, Q., Zhong, W., Jan, Y. N. and Temple, S.** (2002). Asymmetric Numb distribution is critical for asymmetric cell division of mouse cerebral cortical stem cells and neuroblasts. *Development* **129**, 4843-4853.
- Shen, Q., Wang, Y., Dimos, J. T., Fasano, C. A., Phoenix, T. N., Lemischka, I. R., Ivanova, N. B., Stifani, S., Morrisey, E. E. and Temple, S.** (2006). The timing of cortical neurogenesis is encoded within lineages of individual progenitor cells. *Nat. Neurosci.* **9**, 743-751.
- Smart, I. H., Dehay, C., Giroud, P., Berland, M. and Kennedy, H.** (2002). Unique morphological features of the proliferative zones and postmitotic compartments of the neural epithelium giving rise to striate and extrastriate cortex in the monkey. *Cereb. Cortex* **12**, 37-53.
- Solecki, D. J., Model, L., Gaetz, J., Kapoor, T. M. and Hatten, M. E.** (2004). Par6alpha signaling controls glial-guided neuronal migration. *Nat. Neurosci.* **7**, 1195-1203.
- Stricker, S. H., Meiri, K. and Gotz, M.** (2006). P-GAP-43 is enriched in horizontal cell divisions throughout rat cortical development. *Cereb. Cortex* **16** Suppl. 1, i121-i131.
- Takahashi, T., Nowakowski, R. S. and Caviness, V. S., Jr** (1995). Early ontogeny of the secondary proliferative population of the embryonic murine cerebral wall. *J. Neurosci.* **15**, 6058-6068.
- Takahashi, T., Goto, T., Miyama, S., Nowakowski, R. S. and Caviness, V. S., Jr** (1999). Sequence of neuron origin and neocortical laminar fate, relation to cell

- cycle of origin in the developing murine cerebral wall. *J. Neurosci.* **19**, 10357-10371.
- Tamamaki, N., Nakamura, K., Okamoto, K. and Kaneko, T.** (2001). Radial glia is a progenitor of neocortical neurons in the developing cerebral cortex. *Neurosci. Res.* **41**, 51-60.
- Tarabykin, V., Stoykova, A., Usman, N. and Gruss, P.** (2001). Cortical upper layer neurons derive from the subventricular zone as indicated by Svet1 gene expression. *Development* **128**, 1983-1993.
- Tawk, M., Araya, C., Lyons, D. A., Reugels, A. M., Girdler, G. C., Bayley, P. R., Hyde, D. R., Tada, M. and Clarke, J. D.** (2007). A mirror-symmetric cell division that orchestrates neuroepithelial morphogenesis. *Nature* **446**, 797-800.
- von Trotha, J. W., Campos-Ortega, J. A. and Reugels, A. M.** (2006). Apical localization of ASIP/PAR-3:EGFP in zebrafish neuroepithelial cells involves the oligomerization domain CR1, the PDZ domains, and the C-terminal portion of the protein. *Dev. Dyn.* **235**, 967-977.
- Williams, B. P., Read, J. and Price, J.** (1991). The generation of neurons and oligodendrocytes from a common precursor cell. *Neuron* **7**, 685-693.
- Wiznerowicz, M. and Trono, D.** (2003). Conditional suppression of cellular genes: lentivirus vector-mediated drug-inducible RNA interference. *J. Virol.* **77**, 8957-8961.
- Wodarz, A. and Huttner, W. B.** (2003). Asymmetric cell division during neurogenesis in *Drosophila* and vertebrates. *Mech. Dev.* **120**, 1297-1309.
- Wodarz, A., Ramrath, A., Grimm, A. and Knust, E.** (2000). *Drosophila* atypical protein kinase C associates with Bazooka and controls polarity of epithelia and neuroblasts. *J. Cell Biol.* **150**, 1361-1374.
- Wu, S. X., Goebbels, S., Nakamura, K., Nakamura, K., Kometani, K., Minato, N., Kaneko, T., Nave, K. A. and Tamamaki, N.** (2005). Pyramidal neurons of upper cortical layers generated by NEX-positive progenitor cells in the subventricular zone. *Proc. Natl. Acad. Sci. USA* **102**, 17172-17177.
- Yu, F., Kuo, C. T. and Jan, Y. N.** (2006). *Drosophila* neuroblast asymmetric cell division: recent advances and implications for stem cell biology. *Neuron* **51**, 13-20.
- Zimmer, C., Tiveron, M. C., Bodmer, R. and Cremer, H.** (2004). Dynamics of Cux2 expression suggests that an early pool of SVZ precursors is fated to become upper cortical layer neurons. *Cereb. Cortex* **14**, 1408-1420.